



Diagnosing the radiative and chemical contributions to future changes in tropical column ozone with the UM-UKCA chemistry-climate model

James Keeble¹, Ewa M. Bednarz¹, Antara Banerjee², N. Luke Abraham^{1,3}, Neil R. P. Harris⁴, Amanda C. Maycock⁵ and John A. Pyle^{1,3}

¹University of Cambridge, Department of Chemistry, Cambridge, UK

²Department of Applied Physics and Applied Mathematics, Columbia University, New York, NY, USA

³NCAS/University of Cambridge, Department of Chemistry, Cambridge, UK

⁴Centre for Atmospheric Informatics and Emissions Technology, Cranfield University, Cranfield, UK

⁵School of Earth and Environment, University of Leeds, Leeds, UK

Correspondence to: J. Keeble (james.keeble@atm.ch.cam.ac.uk)

Abstract. Chemical and dynamical drivers of trends in tropical total column ozone (TCO₃) for the recent past and future periods are explored using the UM-UKCA chemistry-climate model. A transient 1960-2100 simulation is analysed which follows the representative concentration pathway 6.0 (RCP6.0) emissions scenario for the future. Tropical averaged (10°S-15 10°N) TCO₃ values decrease from the 1970s, reaching a minimum around 2000, and return to their 1980 values around 2040, consistent with the use and emission of ozone depleting substances (ODS), and their later controls under the Montreal Protocol. However, when the ozone column is subdivided into three partial columns (PCO₃) that cover the upper stratosphere (PCO_{3US}), lower stratosphere (PCO_{3LS}) and troposphere (PCO_{3T}), significant differences to the behaviour of the total column are seen. Modelled PCO_{3T} values increase from 1960-2000 before remaining steady under this particular 20 emissions scenario throughout the 21st century. PCO_{3LS} values decrease rapidly from 1960-2000, remain steady until around 2050, before gradually decreasing further to 2100, never recovering to their 1980s values. PCO_{3US} values decrease from 1960-2000, before rapidly increasing throughout the 21st century, recovering to 1980s values by ~2020, and are significantly higher than 1980s values by 2100. Using a series of idealised UM-UKCA time-slice simulations with varying 25 processes that drive the PCO₃ responses in the three regions, and assess how these processes change under different emission scenarios. Finally, we present a simple, linearised model to describe the future evolution of tropical stratospheric column ozone values based on terms representing time-dependent abundances of GHG and ODS.

1 Introduction

Total column ozone (TCO₃) values have a direct effect on human health by preventing harmful ultraviolet (UV) radiation 30 from reaching the surface. It is therefore important to gain a quantitative understanding of how TCO₃ values may evolve



over the 21st century. While ozone mixing ratios are on average highest in the tropical stratosphere, tropical TCO₃ values are the lowest of any region outside of the Antarctic ozone hole (World Meteorological Organization (WMO), 2014). This fact, combined with the high population of many tropical countries, means it is important to understand the various factors that will affect TCO₃ values over the course of the 21st century.

5 The discovery of the ozone hole by Farman et al. (1985) ultimately led to controls on the emissions of CFCs and other ozone-depleting substances (ODS) through the Montreal Protocol and its subsequent amendments (WMO, 2014). As a result, stratospheric concentrations of chlorine are expected to decline throughout the 21st century (e.g. Mäder et al., 2010), and stratospheric ozone concentrations in the mid- and high latitudes are projected to recover to their pre-1980s values (Eyring et al., 2013; WMO, 2014). However, future projections of tropical TCO₃ abundances show a large uncertainty (e.g. Austin et al., 2010; WMO, 2011; 2014), with recent studies indicating that tropical TCO₃ values may not recover to pre-1980s values despite reduction in stratospheric ODS concentrations (e.g. Eyring et al., 2013; Meul et al., 2014).

In the extra-polar stratosphere ozone concentrations are determined by the balance between production and destruction of ozone through gas phase chemical reactions, plus transport into and out of the region of interest (e.g. Brewer and Wilson, 1968; Garny et al., 2011). O_x mixing ratios (where O_x, or odd oxygen, is defined as the sum of ozone (O₃) and atomic oxygen (O)) are determined by sets of photochemical reactions first described by Chapman (1930) plus ozone destroying catalytic cycles involving chlorine, nitrogen, hydrogen and bromine radical species (e.g. Bates and Nicolet, 1950; Crutzen, 1970; Johnston, 1971; Molina and Rowland, 1974; Stolarski and Cicerone, 1974). Unlike in the polar lower stratosphere, heterogeneous processes play only a minor role in determining tropical TCO₃ abundances, although this can change after large volcanic eruptions (e.g. Solomon et al., 1996; Telford et al., 2009) and could also be affected by proposed
20 geoengineering schemes (e.g. Weisenstein et al., 2015; Tang et al., 2016).

Changes in anthropogenic emissions over the course of the 21st century perturb stratospheric ozone chemical cycles involving O_x, ClO_x (Cl+ClO), NO_x (NO+NO₂) and HO_x (OH+HO₂) in two ways. Firstly, the radiative effects of well-mixed GHGs affect both gas phase kinetics and stratospheric dynamics. Secondly, some GHGs, i.e. CFCs, N₂O and CH₄, are also source gases for reactive ClO_x, NO_x and HO_x species.

25 Cooling of the stratosphere due to increased GHG concentrations, particularly CO₂, increases stratospheric ozone concentrations through both increases to the rate constant for the reaction O+O₂+M, leading to an increase of the ratio of O₃ to O, and decreases to the rate constant for the reaction O+O₃ (e.g., Barnett et al., 1974; Haigh and Pyle, 1982; Jonsson et al., 2004). In a similar way, the rate constants for the catalytic loss cycles involving NO_x, HO_x and ClO_x radicals are also temperature dependent (e.g. Brasseur and Hitchman 1988; Randeniya et al., 2002; Rosenfield et al., 2002; Stolarski et al.,
30 2015), and so the efficiency of these cycles for destroying stratospheric ozone is also affected by changes in GHG concentrations.



The climate response to increases in GHG concentrations is expected to include increasing tropopause height, an acceleration of the Brewer-Dobson Circulation (BDC), and changes in the width of the region of the tropical upwelling region (e.g. Butchart et al., 2006, 2010; Garcia et al., 2007; Lorenz and DeWeaver, 2007; Shepherd, 2008; Li and Austin, 2008; Shepherd and McLandress, 2011; Hardiman et al., 2014; Palmeiro et al., 2014). Dynamical changes affect ozone concentrations by directly transporting ozone out of the lower stratosphere (e.g. Plumb, 1996; Avallone and Prather, 1996), and by controlling the amount of reactive Cl_y , NO_y and HO_x that determine the chemical processing of ozone (e.g. Revell et al., 2012, Meul et al., 2014). In addition to the mean advection of airmasses, quasi-horizontal mixing along isentropes is also important for the transport of stratospheric chemical constituents (Hall and Waugh, 1997). However, in the tropics horizontal mixing is weak due to the existence of a sub-tropical transport barrier, the tropical pipe, which acts to some extent to isolate the tropical lower stratosphere from the mid latitudes (Waugh 1996; Neu and Plumb, 1999).

Furthermore, changes to emissions of CFCs, N_2O and CH_4 will alter the concentrations of ClO_x , NO_x , and HO_x radicals, affecting the catalytic cycles that destroy ozone (e.g., Chipperfield and Feng, 2003; Ravishankara et al., 2009). While future stratospheric halogen loadings are expected to decrease throughout the 21st century, emissions of CH_4 and N_2O , which are not regulated in the same way as ODS, are associated with greater uncertainty. The atmospheric concentration of these species, and by extension future concentrations of HO_x and NO_x radicals, is therefore highly sensitive to assumptions made about their future emissions.

Since the photochemical lifetime of ozone is long in the lower stratosphere and short in the upper stratosphere, it is expected that the relative importance of the chemical and dynamical processes described above will vary with altitude, with dynamical changes playing an important role in the lower stratosphere and gas phase chemistry controlling ozone concentrations in the upper stratosphere. This makes it challenging to understand the sources of uncertainty and inter-model differences in future tropical total column ozone trends (e.g. WMO, 2014).

To assess the impacts of future anthropogenic emissions on atmospheric chemistry and climate, a number of representative concentration pathway (RCP) scenarios based on different assumptions about future socio-economic development have been developed (van Vuuren et al., 2011). While stratospheric chlorine loadings are predicted to decrease in the future in all RCP emissions scenarios, emissions of CO_2 , CH_4 and N_2O are associated with greater uncertainty and hence follow a wider range of pathways between the different RCP scenarios (WMO, 2011, 2014; IPCC, 2013; Meinhausen et al., 2011). For example, CH_4 and N_2O emissions are projected to decline during the 21st century in the RCP2.6 scenario, peak around the year 2040/2080 in the RCP4.5/RCP6.0 scenarios respectively, and rise throughout the century in the "business-as-usual" RCP8.5 scenario. The multitude of drivers and processes that affect atmospheric ozone abundances motivates the use of chemistry-climate models (CCMs) to explore how column ozone may evolve over the 21st century under a range of RCP emissions scenarios (e.g. Eyring et al., 2013; Iglesias-Suarez et al., 2016).



Here we present results of a modelling study that assesses projected trends in tropical column ozone. The aims of this paper are to: 1) analyse the contributions from different altitude regions to future tropical column ozone trends; 2) determine the mechanistic drivers of projected tropical column ozone trends using a number of idealised CCM simulations; and 3) formulate a simple model to estimate future tropical column ozone changes and their dependence on the key drivers discussed above. Section 2 describes the CCM simulations used for this study. In section 3, the modelled column ozone trends are discussed and separated into contributions from the upper stratosphere, lower stratosphere and troposphere, before the key drivers of column ozone trends in these separate altitude regions are discussed in section 4. Section 5 presents a discussion on the validity of treating the effects of individual key drivers as additive (i.e. without any co-dependence). In section 6, we produce a simple linear model to describe future tropical stratospheric column ozone changes as a function of GHG and ODS concentrations. Finally, the results are summarized in section 7.

2 Model setup and experimental design

We use version 7.3 of the Met Office's Unified Model HadGEM3-A (Hewitt et al., 2011) coupled with the United Kingdom Chemistry and Aerosol scheme (hereafter referred to as UM-UKCA). The model is run in atmosphere-only mode with a horizontal resolution of 2.5° latitude by 3.75° longitude, 60 vertical levels up to 84 km, and prescribed sea surface temperatures and sea ice extents. For this study, two configurations of UM-UKCA were used which are described below.

An ensemble of transient simulations following the experimental design of the WCRP/SPARC CCM1 REF-C2 experiment (Eyring et al., 2013) was performed using the extended Chemistry of the Stratosphere (CheS+) chemistry scheme. The REF-C2 experiment adopts the RCP6.0 scenario for future GHG and ODS emissions. The CheS+ scheme is an expansion of Morgenstern et al. (2009) in which halogen source gases are considered explicitly, resulting in an additional 9 species, 17 bimolecular and 9 photolytic reactions. CheS+ contains only a simplified tropospheric chemistry scheme. This model was used for the recent SPARC Assessment of Lifetimes (SPARC 2013; Chipperfield et al., 2014) and is described in detail in Bednarz et al. (2016). In total, four ensemble members are used in this study: two simulations run from 1960 to 2099 and two simulations run from 1980 to 2080. The four ensemble members have identical time-dependent boundary conditions, but differ in their atmospheric initial conditions, thereby providing an estimate of internal atmospheric variability. The model is forced at the lower boundary with sea surface temperatures and sea ice fields taken from a parent coupled atmosphere-ocean HadGEM2-ES integration. All transient simulations used in this study include the effects of the 11-year solar cycle in both the radiation and photolysis schemes.

The transient simulations described above include the radiative and chemical effects of changing anthropogenic emissions. In order to separate the relative radiative and chemical contributions to future tropical ozone differences, the transient simulations were supplemented by time-slice simulations performed using the Chemistry of the Stratosphere and Troposphere (CheST) scheme. This scheme is a combination of the UM-UKCA tropospheric (O'Connor et al., 2014) and



stratospheric (Morgenstern et al., 2009) chemical schemes, and is described in detail in Banerjee et al. (2014). Six time-slice experiments were performed using different prescribed GHG and ODS concentrations. The combinations of forcings used for each time-slice integration given in Table 1. Each time-slice was run for 20 years, with the first 10 years discarded as spin-up for the model.

- 5 In order to separate the radiative and chemical responses of ozone abundances to changes in anthropogenic emissions, only the radiative impacts of variations in GHG concentrations and only the chemical effects of changes to ODS concentrations are considered in these simulations. I.e. while differences in GHG concentrations directly affect temperature and circulation, they do not affect the concentration of reactive radical species (e.g. Cl_y , NO_y and HO_x), while the radiative effects of ODS changes are not included. In this study we consider the radiative impact of a large number of GHG species (CO_2 , CH_4 , N_2O ,
10 CFCs) and assume that the dominant driver of chemical changes is changes to ODS loadings. In this way, the chemical impact of changing N_2O and CH_4 emissions is not considered here. The impact of changing GHG concentrations is expressed in terms of differences in Carbon Dioxide Equivalent (CDE; IPCC, 2007).

The time-slice experiments include 3 pairs of simulations with a physical climate state (e.g. SSTs, sea ice, radiative GHG concentrations) commensurate with either year 2000 or 2100 conditions, with year 2100 conditions taken from either the
15 RCP4.5 or RCP8.5 scenarios. Each pair of experiments in turn uses chemical ODS loadings for either the year 2000 or 2100. The time-slice experiments are named accordingly, e.g. $\text{TS}_{2000_{\text{ODS}}}$ includes year 2000 climate conditions and year 2100 ODS loadings, while $\text{TS}_{4.5}$ includes year 2100 climate conditions following the RCP4.5 scenario and year 2000 ODS loadings (see Table 1). A full description of these simulations is provided in Banerjee et al. (2014).

The use of time-slice simulations with different combinations of near-present day and end of century forcings enables the
20 processes that drive projected column ozone trends in the transient experiments to be determined. We purposefully use time-slice experiments with different combinations of forcings to those in the transient simulations (time-slices are run for RCP 4.5 and 8.5 while the transient simulation is run for RCP 6.0), so that we can assess linearities in the ozone response to both ODS and GHG changes.

3 Modelled column ozone trends

- 25 The analysis presented in this study focuses on area weighted averages over 10°S - 10°N . While previous studies of tropical ozone trends have used a broader region to define the tropics, typically from 25°S - 25°N (e.g. Austin et al., 2010; Eyring et al., 2010; Meul et al., 2014), Hardiman et al. (2013) show that, in an ensemble of CMIP5 models following the RCP8.5 scenario, as the magnitude of the tropical upwelling mass flux is projected to increase over the 21st century, the width of the region of upwelling narrows at altitudes below 20 hPa. In order to avoid the impacts of changes to the width of the region
30 of tropical upwelling resulting from increases in GHG concentrations, in this study we use a narrower definition of the



tropics. However, the results presented in this study are not changed significantly when a broader definition of the tropics (30° S- 30° N) is used. In this section, we first describe the changes in tropical total column ozone (defined herein as 0-48 km) and then the partial column trends for the upper and lower stratosphere and the troposphere.

3.1 Total column ozone differences

5 Figure 1 shows tropical averaged TCO₃ anomalies relative to a year 2000±5 averaged value from 1960 to 2100 for each individual ensemble member (grey lines) and the ensemble mean 11-year running mean (black line). The ensemble mean 11-year running mean TCO₃ abundances in the transient simulation are generally anti-correlated with the long-term changes in stratospheric chlorine levels, consistent with other studies (e.g. Eyring et al., 2013). There is a sharp decrease in TCO₃ of ~6 DU from the mid-1970s to 1990, coincident with increases in stratospheric Cl_y concentrations resulting from the emission of ODSs. TCO₃ values remain relatively low from 1990 to 2010, before more gradually recovering to 1980s values by ~2040 and to 1960s values by ~2050, after which they remain relatively constant from 2050-2090. Beyond 2090 there is evidence for further decreases, bringing column values once again below their 1980s values. This behaviour is broadly consistent with previous studies (e.g. Oman et al., 2010; Eyring et al., 2013; Meul et al., 2014). Superimposed on the TCO₃ 11-year running mean is the signal of the 11-year solar cycle, which leads to variations of <5 DU between solar maximum and minimum. The large degree of natural variability simulated in the model highlights the difficulties in assessing ozone trends and return dates from relatively short observational records (as discussed in Harris et al., 2015).

The time-slice experiments, plotted in Figure 1 as discrete points (circles and triangles), show the dependence on the RCP scenario of modelled year 2100 tropical TCO₃ values. Tropical TCO₃ increases by around 12 DU when stratospheric Cl_y loadings are decreased from their year 2000 values to year 2100 values under fixed year 2000 GHG conditions (TS2000 - TS2000_{ODS}, shown by the difference in the green symbols in Figure 1). However, the same decrease in stratospheric Cl_y abundances leads to slightly smaller increases in tropical TCO₃ when future changes in climate are also included according to the RCP4.5 or RCP8.5 scenario (11 DU for TS4.5 – TS4.5_{ODS} and 10 DU for TS8.5 – TS8.5_{ODS}, shown by the blue and red symbols in Fig. 1, respectively). The climate dependence of the effect of a reduction in ODS results from the temperature dependence of ClO_x radical chemistry on ozone destruction (e.g. Haigh and Pyle, 1982). The effect of future radiative changes resulting from increases in GHGs, and the associated changes in climate state, on TCO₃ is explored by comparing the TS4.5 and TS8.5 time-slice simulations with TS2000. Under a more moderate increase in GHG concentrations (TS4.5 - TS2000, green to blue circles Figure 1), tropical TCO₃ increases by 4.0 DU between year 2000 and 2100, while under a much larger GHG concentration change (TS8.5 - TS2000, green to red circles Figure 1), tropical TCO₃ values show no change, indicating a non-linear response to the magnitude of GHG forcing (Banerjee et al., 2016).



3.2 Partial column differences

Projected trends in tropical ozone concentrations show a complex vertical structure. In this section we assess modelled changes in ozone partial columns (PCO₃) for the upper stratosphere (30–48 km; PCO_{3US}), lower stratosphere (tropopause to 30 km; PCO_{3LS}) and troposphere (PCO_{3T}). Note that we employ a scenario-consistent tropopause height to calculate the partial columns, as defined by the lapse rate (WMO, 1957) within each experiment, rather than a fixed height definition. Thus, any changes in tropopause height will affect the lower stratosphere and tropospheric partial columns even if the vertical distribution of ozone concentrations is unchanged.

PCO_{3US} values decrease by around 4 DU from 1960 to the late 1990s (Figure 2a), consistent with the increasing stratospheric Cl_y concentrations over this period. From around 2000 onwards, PCO_{3US} values increase rapidly, returning to 1980 values by ~2020, and 1960 values by ~2040. From 2040, PCO_{3US} values continue to increase to around 3–4 DU above their 1960s values by 2100 – the well-known ozone “super recovery” effect (Chipperfield and Feng, 2003).

The time-slice experiments show that an increase in PCO_{3US} values of 5 DU can be attributed to Cl_y changes over the 21st century (calculated as the difference between the green symbols in Figure 2a). As well as responding to changes in stratospheric Cl_y, PCO_{3US} values in the late 21st century is dependent on the RCP scenario followed, which determines the magnitude of stratospheric cooling (Maycock, 2016). PCO_{3US} for TS4.5 and TS8.5, which consider only the radiative effects of changes in GHGs, both show higher values than TS2000 (+5 DU for TS4.5 and +12 DU for TS8.5). These results can be used to calculate an approximate change in tropical PCO_{3US} abundance per unit change in CDE and EESC concentration, which gives values of $\frac{\Delta PCO_{3US}}{\Delta CDE} \approx 0.02 \text{ DU ppmv}^{-1}$ and $\frac{\Delta PCO_{3US}}{\Delta EESC} \approx -1.72 \text{ DU ppbv}^{-1}$. These results indicate that over the recent past upper stratospheric ozone depletion resulting from increased Cl_y concentrations has in part been offset by radiative cooling resulting from increased GHG concentrations, and that in the future both increased GHG concentrations and reduced stratospheric Cl_y will result in increases in upper stratospheric ozone concentrations. However, as discussed for TCO₃, the impact of ODS changes on upper stratospheric partial column abundance is dependent on GHG concentrations (Figure 2a).

As was found in the upper stratosphere, the modelled historical trend in PCO_{3LS} is strongly negative, with a decrease of ~6 DU from 1960 to the late 1990s (Figure 2b). However, the projected future trends in PCO_{3LS} differ greatly from those in the upper stratosphere. From 2000 to ~2050, modelled PCO_{3LS} abundances remain steady, before again decreasing during the latter half of the 21st century.

The time slice experiments demonstrate the competing effects of decreasing stratospheric Cl_y and the radiative changes following increasing GHG concentrations on ozone in the tropical lower stratosphere over the course of the 21st century. As in the upper stratosphere, projected decreases in stratospheric Cl_y result in increases to PCO_{3LS} values (compare green



triangle and circle in Figure 2b). However, radiative changes following increases in GHG concentrations lead to decreases in PCO_{3LS} values (compare blue/red circles with green circle in Figure 2b). For changes in GHGs alone, the magnitude of the lower stratospheric partial column ozone response increases with the magnitude of the CDE perturbation (-4 DU for TS4.5-TS2000, -16 DU for TS8.5-TS2000). As for upper stratospheric partial column values, changes to tropical PCO_{3LS} values per unit change in CDE and EESC concentrations can be calculated, giving $\frac{\Delta PCO_{3LS}}{\Delta CDE} \approx -0.03 \text{ DU ppmv}^{-1}$ and $\frac{\Delta PCO_{3LS}}{\Delta EESC} \approx -1.92 \text{ DU ppbv}^{-1}$. In comparison to the upper stratosphere, while past increases in stratospheric Cl_y and GHG concentrations have led to decreased lower stratospheric ozone concentrations, in the future ozone recovery resulting from decreased stratospheric Cl_y will compete with ozone decreases resulting from increased GHG concentrations. As was seen for the upper stratosphere, the PCO_{3LS} response to a given decrease in ODS is dependent on the GHG concentration, (+7 DU for TS2000_{ODS} - TS2000, +6 DU for TS4.5_{ODS} - TS4.5 and +4 DU for TS8.5_{ODS} - TS8.5).

From 1960 to 2000, the tropical tropospheric partial ozone column increases by approximately 5 DU (Figure 2c), then remains constant until 2040, before increasing again by ~2 DU by 2060. There is some evidence from the transient simulations that tropical tropospheric partial ozone column values decrease to year 2000 values during the final decade of the 21st century. The time-slice experiments indicate that tropical tropospheric column ozone is relatively insensitive to differences in GHGs for the two RCP scenarios considered here, with values in TS4.5 and TS8.5 both increasing by ~5 DU. As expected, tropical tropospheric column ozone shows no significant response to changes in ODS concentrations irrespective of the GHG loading. Note that the time-slice simulations do not explore the role of tropospheric CH_4 , NO_x and volatile organic compounds (VOCs), which are likely to be important drivers of tropospheric ozone changes in the transient simulations; their likely roles are discussed in Section 4.3.

20 4 Drivers of column ozone changes

As discussed above, both ODS and GHG concentrations drive ozone changes in the upper stratosphere, lower stratosphere and troposphere. However, while decreases in ODS result in increases in ozone throughout the stratosphere, increases in GHGs drive increases in upper stratospheric partial column ozone, but decreases in lower stratospheric partial column ozone. The contrasting impacts of these forcings as a function of altitude reflect the various chemical and transport processes that control ozone abundances in different regions. In the following sections the major mechanisms operating in each of the three partial column regimes are explored.

4.1 Upper Stratosphere

As discussed in Section 3.2, PCO_{3US} values are projected to recover quickly to pre-1980 values over the next few decades and to continue to increase throughout the 21st century, leading to super-recovery of the partial column by 2100 (Figure 2a). The upper rows in Table 2 give values for the TS2000, TS2000_{ODS}, TS4.5 and TS8.5 simulations of PCO_{3US} abundances,



chemical loss of O_x through reactions with each of the key chemical families (halogens, HO_x , NO_x , and O_x), chemical production and O_x lifetime. The simulated upper stratospheric partial ozone column under near present day conditions (TS2000) is 62 DU. Net chemical loss is 48 DU day⁻¹, with the major loss being due to catalytic cycles involving NO_x (39%), with smaller contributions from HO_x (22%), halogens (20%) and O_x (19%). The average chemical lifetime of ozone
5 in the tropical upper stratosphere (calculated as the burden divided by net chemical loss) is 1.3 days. These results are consistent with previous studies (e.g. WMO, 1998; Grooß et al., 1999; Meul et al., 2014).

PCO_{3US} , as a function of stratospheric EESC at 45km, for both the time-slice and transient simulations is shown in Figure 3. Annual mean values for the transient simulations covering 1960-2100 are shown as crosses, with different colours denoting different 20 year sections of the simulations. From 1960 to 2000, as EESC concentrations rapidly increase by ~3 ppbv,
10 PCO_{3US} abundances decrease by ~3 DU. From 2000-2100, as EESC concentrations decrease, PCO_{3US} abundances are projected to increase, although the trend from 2000 to 2100 does not retrace the trend from 1960 to 2000, as highlighted by the shaded points for the transient simulations. Instead, the transient simulations indicate a larger change in PCO_{3US} per unit change in ODS in the future compared to the past owing to the increasing GHG concentrations (i.e. the "super-recovery" of ozone).

15 The time-slice experiments can be used to quantify the radiative effects of GHG increases and the chemical effects of ODS on PCO_{3US} changes. Comparison of $TS2000_{ODS}$ with TS2000 isolates the effects of future changes in ODSs on PCO_{3US} ; as discussed in Section 3.2, we find that reductions in EESC increase PCO_{3US} abundances by 5 DU (8%). Table 2 shows that net chemical O_x loss in $TS2000_{ODS}$ is reduced by 5% compared to TS2000, driven predominantly by large decreases in O_x loss through catalytic cycles involving halogens, which are reduced by 63%. O_x loss through reactions with HO_x , NO_x and
20 O_x all increase, predominantly due to the increase in ozone concentrations, but also due to temperature changes, which are themselves a response to increases in ozone (e.g. Shine et al., 2003). The upper stratosphere warms by ~2 K (Figure 4) when GHGs are held constant, consistent with the multi-model results presented by Maycock (2016). The reaction $O+O_3$ has a strong temperature dependence and becomes faster at higher temperatures, thereby further increasing O_x loss in $TS2000_{ODS}$ relative to TS2000. Reactions involving HO_x and NO_x have weaker temperature dependencies, and show smaller increases.

25 In addition to the reductions in EESC, the cooling of the stratosphere induced by increased GHG concentrations (mainly CO_2) will be a major driver of future PCO_{3US} changes. Comparison of TS8.5 with TS2000 quantifies the impact of GHG changes alone on PCO_{3US} . As the chemical lifetime of O_x is short in the upper stratosphere, transport changes are expected to have a relatively minimal effect on projected trends. Instead, PCO_{3US} changes are driven by the response of reaction rates to the simulated temperature changes. The tropical upper stratosphere in TS8.5 is ~11 K cooler than in TS2000 (see
30 Banerjee et al., 2016). This leads to a PCO_{3US} increase of 12 DU (21%), which is driven predominantly by a decrease in the reaction $O+O_3$, but also by a change in partitioning of O_x due to the acceleration of the reaction $O+O_2+M \rightarrow O_3+M$ (Jonsson et al., 2004; Banerjee et al., 2016).



The relationship between $\text{PCO}_{3\text{US}}$ and temperature for the transient and time-slice experiments is shown in Figure 4. From 1960 to 2000, temperatures and $\text{PCO}_{3\text{US}}$ both decrease. The ozone decreases are driven predominantly by increasing ODSs, which deplete ozone chemically. Decreased ozone concentrations in turn reduce upper stratospheric heating, thereby reducing temperatures (e.g. Forster and Shine, 1997; Shine et al., 2003). From 2000 to 2100, as temperatures decrease further, mainly due to cooling from increased GHG abundances, ozone concentrations increase, driven predominantly, as discussed above, by a reduced rate for the reaction of $\text{O}+\text{O}_3$ and decreased ODS concentrations. These increases in ozone offset part of the stratospheric cooling due to rising GHG concentrations (Maycock, 2016). The impact of temperature on $\text{PCO}_{3\text{US}}$ can be isolated by fitting lines through the sets of time-slice experiments with the same ODS loadings (i.e. TS2000, TS4.5 and TS8.5). We find that the upper stratospheric ozone column increases by $\sim 1 \text{ DU K}^{-1}$, which, when combined with decreasing ODS, drives the super recovery of $\text{PCO}_{3\text{US}}$.

4.2 Lower Stratosphere

In comparison to the upper stratosphere, the chemical lifetime of O_x in the tropical lower stratosphere is long (>1 month, see lower rows in Table 2), so dynamical processes play a much more important role in determining ozone abundances there. A strengthening of the BDC, which is projected to occur in the future in response to increasing in GHGs (e.g. Shepherd and McLandress, 2011; Hardiman et al., 2014; Palmeiro et al., 2014), would therefore have a significant effect on tropical lower stratospheric ozone. We use the Transformed Eulerian Mean residual vertical velocity ($\overline{w^*}$; Andrews et al., 1987) at 70 hPa as a measure of the strength of the advective part of the BDC. In the transient REF-C2 simulations, the annual and tropical (10°S - 10°N) mean $\overline{w^*}$ at 70 hPa increases by around 20% from $\sim 0.20 \text{ mm s}^{-1}$ in 1960 to $\sim 0.24 \text{ mm s}^{-1}$ in 2100.

Consistent with the important role of the BDC in determining tropical lower stratospheric ozone abundances, there is a strong negative correlation ($r=-0.76$) between $\text{PCO}_{3\text{LS}}$ and $\overline{w^*}$ at 70hPa (Figure 5a). By plotting $\overline{w^*}$ vs. CDE concentration as a function of time (Figure 5b) and comparing time-slice runs with constant ODS loadings (i.e. TS2000, TS4.5 and TS8.5) an approximate value for the acceleration of the BDC per unit increase in CDE can be calculated. From these experiments, a value of $2 \times 10^{-4} \text{ mm s}^{-1} \text{ ppmv}^{-1}$ is calculated. By comparison, the chemical effects of changes in ODS concentrations also impact on the modelled strength of the BDC by $5.4 \times 10^{-3} \text{ mm s}^{-1} \text{ ppbv}^{-1}$. This indicates that, per molecule, ODS increases have a greater effect on the BDC than GHGs. Previous work using the UM-UKCA model has indicated that an acceleration in stratospheric circulation, particularly the lowermost branch of the BDC, is to be expected from increased polar lower stratospheric ozone depletion and the resulting increase in meridional temperature gradients (Keeble et al., 2014; Braesicke et al., 2014). Our results also corroborate the findings of Polvani and Wang (2017) who highlight the dominant impact of ODS on tropical lower stratospheric temperature and ozone through changes in tropical upwelling between 1960-2000. Results from this study suggest future recovery of polar lower stratospheric ozone will act to slow the BDC, partly offsetting the acceleration expected due to increased GHG concentrations.



The combined influence of GHGs and ODS on the strength of tropical upwelling can largely explain the three distinct periods of behaviour in tropical $\text{PCO}_{3\text{LS}}$ seen in Figure 2b. Firstly, between 1960-2000, the partial column shows the largest rate of change as the effect of GHGs and ODS on tropical upwelling reinforce one another, both strengthening the tropical upwelling and reducing $\text{PCO}_{3\text{LS}}$. Secondly, between 2000-2040, ODS reductions (and the associated polar ozone recovery) and increasing GHGs compete in their effects on tropical upwelling and the partial column, which remains relatively constant during this time. Finally, between 2040-2100, by which time the ODS influence on ozone has already been reduced significantly, the effect of GHGs on tropical upwelling dominates and $\text{PCO}_{3\text{LS}}$ values again show a decreasing trend.

Finally, we note that in addition to changing to the strength of the BDC, increasing GHG concentrations also affect $\text{PCO}_{3\text{LS}}$ values by decreasing chemical production as a result of increased overhead column ozone (see Section 4.1). Table 2 shows how O_x production in the lower stratosphere responds to changes in ODS and CDE concentrations. Compared to TS2000, lower stratospheric O_x production in TS2000_{ODS} and TS8.5 has decreased, consistent with the increased partial column abundances in the upper stratosphere in these simulations. Using this information we can calculate the response of lower stratospheric O_x production to changes in upper stratospheric partial column abundance; we estimate that tropical lower stratospheric O_x production will decrease by 0.1 DU day^{-1} for each additional DU of ozone in the upper stratosphere.

4.3 Troposphere

The primary factors affecting future tropospheric ozone are likely to be changes in the emission of ozone precursors (CH_4 , NO_x and VOCs) and changes in climate. Changes in climate can affect tropospheric ozone abundances in several ways, including changes in water vapour amounts, lightning NO_x emissions (LNO_x) and stratosphere-troposphere exchange of ozone (STE) (e.g. Thompson et al., 1989; Young et al., 2013; Banerjee et al., 2016). Future ODS-driven stratospheric ozone recovery is also projected to increase tropospheric ozone abundances through STE (e.g. Zeng and Pyle, 2003; Banerjee et al., 2016). Here, we first use the time-slice simulations to deduce the role of climate change and ozone recovery on future tropospheric column ozone changes. Then, we discuss the likely drivers of the partial column evolution between 1960-2000 in the transient simulations, where changes in ozone precursors must also be considered.

Climate change resulting from changing concentrations of CO_2 in the TS4.5 and TS8.5 experiments enhances tropical tropospheric column ozone by around 4 DU relative to TS2000. The increases are driven primarily by LNO_x , which increases by 2 and $4.7 \text{ Tg(N) yr}^{-1}$ under the RCP4.5 and RCP8.5 scenarios, respectively (Banerjee et al., 2014). In fact, a further sensitivity experiment in which climate is allowed to change according to the RCP8.5 forcings, but LNO_x is kept fixed at TS2000 values (not otherwise discussed; see Banerjee et al., 2014) shows a 3 DU decrease in tropospheric column ozone. The reduction arises from increases in tropospheric humidity under a warming climate (e.g. Thompson et al., 1989). Thus, the increase in LNO_x at RCP8.5 contributes 7 DU to the increase in tropospheric column ozone.



A further increase in the tropospheric partial column arises from the increase in the height of the tropopause under a warmer climate. In the ensemble mean of the transient simulations (which follow the RCP6 scenario), the tropopause height increases by 800m from ~16.1 km in the year 2000 to ~16.9 km in the year 2100. The impacts of increasing tropopause height on tropospheric column ozone are calculated as the difference between the full tropospheric column from the column values calculated using the year 2000 tropopause height of 16.1 km. This analysis indicates that tropopause height increase between 2000-2100 accounts for ~1.5 DU of the increase in the total tropospheric column.

In contrast to the effects of climate change, reductions in ODS primarily affect tropospheric ozone in the extratropics through STE (Banerjee et al., 2016). Conversely, in the tropics, ODS have little impact on tropospheric ozone, with the partial column increasing by <1 DU in the TS2000_{ODS} experiment compared to TS2000.

The time-slice sensitivity experiments suggest that climate change acts to increase tropospheric column ozone in the transient simulations. As discussed above, an additional consideration in the transient simulations (that are run under all-forcings at RCP6.0) are changes in ozone precursors, which here include CH₄, CO and NO_x. The largest rate of change for tropospheric column ozone occurs over the recent past (1960-2000) (Figure 2c), when increases in anthropogenic NO_x emissions (Lamarque et al., 2010) drive increases in ozone production. After 2000, all RCP scenarios project reductions in anthropogenic NO_x and NMVOC emissions (Meinhausen et al., 2011), which would drive tropospheric ozone reductions. However, tropospheric column ozone remains steady up to ~2040, partly due to the compensating effects of climate change, as suggested by the time-slice simulations, but also due to increasing tropospheric CH₄ concentrations (Revell et al., 2015). The rise in tropospheric column ozone until 2060-2080 and its subsequent decline is consistent with the evolution of CH₄, which maximises around 2080 at RCP6.0.

5 Developing a simple model for predicting stratospheric column ozone change in the tropics

Future projections of total column ozone are strongly dependent on the assumed pathway for anthropogenic emissions, for which there is a great deal of uncertainty, particularly in relation to emissions of CO₂, CH₄ and N₂O. CCMs are commonly used to assess possible future changes in ozone under a small number of well-defined scenarios, e.g. the Representative Concentration Pathways (RCP; van Vuuren et al., 2011) used in the IPCC Fifth Assessment Report. These emissions scenarios are neither forecasts nor policy recommendations, but instead are chosen to represent a range of possible global socio-economic and technological pathways for the future. In order to comprehensively quantify the response of the chemistry-climate system to such emissions scenarios, long, computationally expensive model simulations are required. However, simpler models can also be used to identify which processes dominate future trends and to explore the composition response to a wider range of emissions scenarios.



In Section 4 we showed that future changes in tropical stratospheric column ozone are driven primarily by changes in: (i) the halogen-catalysed loss; (ii) the strength of tropical upwelling; and (iii) the upper stratospheric cooling induced by GHGs (mainly CO₂). Furthermore, the partial column ozone trends were found to be, to first order, linearly dependent on ODS and CDE concentrations. This conclusion was derived from transient runs based on a single emissions scenario and multiple
5 time-slice runs based on 3 additional scenarios, and so is valid for a range of possible CDE and ODS concentrations. In this section, we describe a simple, computationally inexpensive linearised model that can be used to estimate tropical stratospheric column ozone changes under a much wider range of future emission scenarios than are typically explored by comprehensive CCMs (e.g. Morgenstern et al., 2017).

The simplest version of such a model has a linear dependence of stratospheric column ozone (SCO3) on GHG concentrations
10 (expressed in CDE) and ODS. We justify this simple approach based on the approximately linear dependencies of ozone found in UM-UKCA and shown in Figure 3 and Figure 5. Such a model has the form:

$$SCO3_t = SCO3_{t_0} + \left(\frac{\Delta SCO3}{\Delta CDE} \cdot (CDE_t - CDE_{t_0}) \right) + \left(\frac{\Delta SCO3}{\Delta ODS} \cdot (ODS_t - ODS_{t_0}) \right), \quad (1)$$

where the subscripts t_0 and t signify the reference year and the year the model is solving for, respectively. The constants $\frac{\Delta SCO3}{\Delta CDE}$ and $\frac{\Delta SCO3}{\Delta ODS}$, which represent the SCO3 change due to CDE and ODS perturbations, respectively, can be calculated using
15 the time-slice simulations, as these simulations perturb ODS and GHGs separately. $\frac{\Delta SCO3}{\Delta ODS}$ was calculated by averaging the values obtained from the three pairs of simulations with different ODS loadings, but the same CO₂ mixing ratios. The term $\frac{\Delta SCO3}{\Delta CDE}$ was calculated by averaging the linear fits through the two sets of three simulations with the same ODS loading, but different GHG mixing ratios. Using this method, values of $\frac{\Delta SCO3}{\Delta CDE} = -0.005$ DU ppmv⁻¹ and $\frac{\Delta SCO3}{\Delta ODS} = -3.64$ DU ppbv⁻¹ were
20 obtained. The simple model is therefore trained using the time-slice simulations and can then be compared against the transient simulations in order to determine its ability to reproduce output from the same comprehensive CCM under a different scenario. These comparisons are shown in Figure 7 for the RCP4.5, 6.0 and 8.5 scenarios alongside annual mean stratospheric ozone column values from the transient UM-UKCA RCP6.0 simulations.

Projections of SCO3 made using the simple model following the RCP6.0 scenario for GHG and ODS (purple line, Figure 7) can be compared with the fully-coupled RCP6.0 transient simulations (grey lines, Figure 7). Overall the agreement between
25 the simple model and the fully-coupled CCM is reasonable and confirms that the major drivers of future tropical SCO3 change are the emissions of GHGs and ODS. However, it is also surprising as the atmospheric processes involved are complex and, in many cases, non-linear. For example, the changes in HO_x and NO_x chemistry resulting from future changes in CH₄ and N₂O emissions would appear to be of second order on the timescales considered. Similarly, the dynamic feedbacks resulting from increasing vertical velocities on radical production from N₂O, CFCs and CH₄ are limited in



magnitude. One of the reasons for this is most likely the limited latitude range of the region studied. The effects of increasing N_2O and CH_4 concentrations on ozone destruction are expected to increase with latitude (e.g. Revell et al., 2012), while the effects of dynamical feedbacks are more likely to appear at the edge of the tropical pipe or at low altitudes due to branching in the BDC (e.g. Garny et al., 2011).

- 5 As well as using the simple model to calculate SCO_3 projections under the RCP6.0 scenario, additional emissions scenarios have also been investigated. These scenarios include RCP4.5, RCP8.5, RCP6.0 using ODS fixed at 1960 values and RCP6.0 using CDE fixed at 1960 values. Projected SCO_3 values for each of these scenarios are shown in Figure 7. It should be noted that the SCO_3 projections calculated are sensitive to the point at which they are initialised. Figure 7 shows a number of scenarios initialised from 1960s SCO_3 values taken from the transient simulations.
- 10 Caveats exist for developing and using such simple models. The constants $\frac{\Delta\text{SCO}_3}{\Delta\text{CDE}}$ and $\frac{\Delta\text{SCO}_3}{\Delta\text{ODS}}$ likely vary with latitude, and so those calculated for this study could not be used for projections of extratropical stratospheric column values. Furthermore, they are likely to vary between different CCMs. Indeed, differences between these values in different CCMs would indicate varying sensitivities to CO_2 and ODS changes and may help in the identification of which processes have high uncertainty and should be explored in more detail.
- 15 The aim of such a model is not to replace fully-coupled CCMs, but to provide a simple and computationally inexpensive way of exploring possible future SCO_3 changes in the tropics. In this capacity, it appears to offer considerable promise and could act as a valuable complementary approach to the 2D model studies which are currently used to investigate multiple scenarios (Fleming et al., 2011; WMO, 2014).

6 Conclusions

- 20 We have investigated the drivers of past and future changes in tropical averaged total column ozone using a number of model runs performed with two versions of the UM-UKCA model. Four transient simulations following an RCP6.0 future emissions scenario were performed, with the longest of these simulations spanning the period 1960-2100. These runs were supplemented with 6 time-slice experiments run under a range of prescribed GHG and ODS loadings commensurate with either year 2000 or 2100 levels. Note that in the time-slice experiments only the chemical impacts of changes to ODS
- 25 loadings and only the radiative impacts of GHG perturbations are considered, and so we are able to separate the chemical and radiative drivers of future tropical ozone column changes. Changes in tropical total column ozone were split into three partial columns based on altitude: the troposphere, the lower stratosphere (tropopause to 30km) and the upper stratosphere (30-48km). Future stratospheric ozone projections for each of these regions are governed by different processes and thus show distinct behaviours.



Future tropospheric ozone changes are driven by a number of processes, including changes to surface emissions of ozone precursors such as CH_4 and NO_x , increased NO_x emissions from lightning associated with increasing GHG concentrations, and changes to troposphere height. There is a high level of uncertainty associated with future emissions of ozone precursors, linked to uncertainties in anthropogenic emissions, biomass burning and land use changes. While the various RCP scenarios follow a range of future emissions scenarios for many key tropospheric ozone precursors, particularly CH_4 , further work is required to explore the impact of changes to tropospheric ozone on TCO_3 trends during the 21st century in order to understand to what extent changes in tropospheric ozone column offset decreases in the lower stratosphere.

In the simulations described in this study, it has been shown that projected changes to stratospheric ozone throughout the 21st century are predominantly driven by chemical changes resulting from differences in ODS loadings and radiative changes resulting from differences in GHG mixing ratios. The transient UM-UKCA simulations run under the RCP6.0 emissions scenario show that by the year 2100 stratospheric column ozone values are increased by 5 DU from the minimum values around the year 2000. However, modelled stratospheric column values in the simulations never recover to 1960s values despite declining stratospheric ODS loadings, due to the competing effects of changes in partial column ozone values in the lower and upper stratosphere.

Chemical and radiative perturbations drive changes to stratospheric ozone abundances in both the upper and lower stratospheric partial columns. However, while in the upper stratosphere both reducing ODS concentrations and increasing GHG concentrations lead to increased ozone abundances, in the lower stratosphere decreasing ODS concentrations, which lead to increased ozone abundances, are counteracted by the effects of increased GHG concentrations, which lead to decreased ozone abundances. Furthermore, while in the upper stratosphere GHG and ODS increases lead to chemical changes (by changing gas phase kinetics and the concentration of EESC respectively) which dominate the projection of ozone abundances, in the lower stratosphere ozone differences are the result of changes to the strength of the BDC, which accelerates in response to future GHG increases and decelerates in response to future ODS decreases.

Changes to lower stratospheric ozone, where the chemical lifetime of ozone is typically >1 month, are controlled predominantly by changes to transport. Projected increases in GHGs lead to an acceleration of the BDC, which is associated with increased transport of relatively ozone poor air masses into the tropical lower stratosphere, thereby decreasing ozone mixing ratios and the partial lower stratospheric column ozone. The magnitude of acceleration of the BDC is highly correlated with increasing GHG mixing ratios, and so the total effect of transport changes on tropical lower stratospheric ozone depends strongly on the future GHG emissions scenario. Future reductions in lower stratospheric ozone partial column values also result from decreased production of O_x from photolysis of O_2 in the lower stratosphere due to increased overhead ozone concentrations in the upper stratosphere. Analysis of the simulations presented here suggests lower stratospheric O_x production will decrease by 0.1 DU day^{-1} for each additional DU of ozone in the upper stratosphere.



Future concentrations of ozone in the upper stratosphere are driven by changes in both ODS loading and temperature. In contrast to the lower stratosphere, both CO₂ increases and ODS decreases lead to increased ozone concentrations. ODS concentrations are expected to decrease throughout the 21st century due to the restrictions on ODS emissions imposed by the Montreal Protocol and its amendments. At the same time, stratospheric GHG concentrations, particularly CO₂, are projected to increase, leading to stronger radiative cooling of the stratosphere and slowing of the temperature dependent ozone loss cycles, particularly those of the Chapman cycle. The combination of these two effects is expected to lead to super-recovery of upper stratospheric partial column values above their 1960s values.

Projections of stratospheric column ozone values in the tropics are therefore the result of a complex interplay between ozone trends in the lower and upper stratosphere. Understanding the extent to which dynamically induced decreases in lower stratospheric partial column values counteract upper stratospheric super-recovery is key to making accurate projections of stratospheric column ozone, and requires detailed modelling of both photochemical and dynamical processes under a range of future emissions scenarios. However, output produced by complex, fully-coupled CCMs can be used to create simple linear models which can be used to explore the stratospheric ozone column response to changing surface GHG and ODS concentrations. Simple linear models are computationally inexpensive and can be used to investigate a wide range of emission scenarios much more quickly than ensembles of fully-coupled CCMs. In this work we present a simple linearised model which has been developed to help investigate projections of stratospheric column ozone following different future emissions scenarios. The model includes terms for the dependence of stratospheric column ozone on ODS and CDE mixing ratios. The simple model was trained using data from the single and combined forcing time-slice UM-UKCA experiments and then its performance compared against the transient model simulations. Good agreement was found between the simple model and the long-term behaviour in the fully-coupled CCM simulations, confirming emissions of GHG and ODS to be the major drivers of long-term future tropical stratospheric column ozone changes. Results from the simple model indicate stratospheric column ozone changes resulting from future CH₄ and N₂O emissions are of second order on the timescales considered here.

While fully-coupled CCM simulations are required to quantify changes in, and identify the processes responsible for, future atmospheric composition changes, simple models can provide a complementary approach for investigating a broad range of potential emissions scenarios. Furthermore, it is hoped that the model presented here can be further developed to include more parameters (e.g. N₂O, CH₄) by performing more simulations, and also to more accurately constrain the terms of the simple model by using simulations from more CCMs. This would also allow for a better assessment of the uncertainty of each of the terms used in the simple model.



Acknowledgements

The research leading to these results has received funding from the European Community's Seventh Framework Programme (FP7/2007 - 2013) under grant agreement n° 603557 (StratoClim), the European Research Council through the ACCI project (project number: 267760), the Natural Environment Research Council through the CAST project (NE/ I030054/1) and
5 ACM's Independent Research Fellowship (NE/M018199/1). We thank NCAS-CMS for modelling support. Model simulations have been performed using the ARCHER UK National Supercomputing Service and MONSooN system, a collaborative facility supplied under the Joint Weather and Climate Research Programme, which is a strategic partnership between the UK Met Office and the NERC.

References

- 10 Andrews, D. G., Holton, J. R., and Leovy, C. B.: Middle Atmosphere Dynamics, Academic Press, Orlando, Florida, 489 pp., 1987.
- Austin, J., Scinocca, J., Plummer, D., Oman, L., Waugh, D., Akiyoshi, H., Bekki, S., Braesicke, P., Butchart, N., Chipperfield, M., Cugnet, D., Dameris, M., Dhomse, S., Eyring, V., Frith, S., Garcia, R. R., Garny, H., Gettelman, A., Hardiman, S. C., Kinnison, D., Lamarque, J. F., Mancini, E., Marchand, M., Michou, M., Morgenstern, O.,
15 Nakamura, T., Pawson, S., Pitari, G., Pyle, J., Rozanov, E., Shepherd, T. G., Shibata, K., Teyssèdre, H., Wilson, R. J., and Yamashita, Y.: Decline and recovery of total column ozone using a multimodel time series analysis, *J. Geophys. Res.*, 115, D00M10, doi:10.1029/2010JD013857, 2010.
- Avallone, L. M. and Prather, M. J.: Photochemical evolution of ozone in the lower tropical stratosphere, *J. Geophys. Res.*, 101, 1457–1461, doi:10.1029/95JD03010, 1996.
- 20 Banerjee, A., Archibald, A. T., Maycock, A. C., Telford, P., Abraham, N. L., Yang, X., Braesicke, P., and Pyle, J. A.: Lightning NO_x, a key chemistry–climate interaction: impacts of future climate change and consequences for tropospheric oxidising capacity, *Atmos. Chem. Phys.*, 14, 9871–9881, doi:10.5194/acp-14-9871-2014, 2014.
- Banerjee, A., Maycock, A. C., Archibald, A. T., Abraham, N. L., Telford, P., Braesicke, P., and Pyle, J. A.: Drivers of changes in stratospheric and tropospheric ozone between year 2000 and 2100, *Atmos. Chem. Phys.*, 16, 2727–2746,
25 doi:10.5194/acp-16-2727-2016, 2016.
- Barnett, J. J., Houghton, J. T., and Pyle, J. A.: The temperature dependence of the ozone concentration near the stratopause, *Q. J. Roy. Meteor. Soc.*, 101, 245–257, 1974.
- Bates, D. R. and Nicolet, M.: The photochemistry of atmospheric water vapor, *J. Geophys. Res.*, 55, 01–327, doi:10.1029/JZ055i003p00301, 1950.
- 30 Bednarz, E. M., Maycock, A. C., Abraham, N. L., Braesicke, P., Dessens, O., and Pyle, J. A.: Future Arctic ozone recovery: the importance of chemistry and dynamics, *Atmos. Chem. Phys.*, 16, 12159–12176, doi:10.5194/acp-16-12159-2016, 2016.



- Braesicke, P., Keeble, J., Yang, X., Stiller, G., Kellmann, S., Abraham, N. L., Archibald, A., Telford, P., and Pyle, J. A.: Circulation anomalies in the Southern Hemisphere and ozone changes, *Atmos. Chem. Phys.*, 13, 10677-10688, doi:10.5194/acp-13-10677-2013, 2013.
- Brasseur, G. and Hitchman, M. H.: Stratospheric response to trace gas perturbations: Changes in ozone and temperature distributions, *Science*, 240, 634–637, 1988.
- 5 Brewer, A. W. and Wilson, A. W.: The regions of formation of atmospheric ozone, *Quarterly J. R. Meteorol. Soc.*, 94: 249-265. doi: 10.1002/qj.49709440103, 1968
- Butchart, N., Scaife, A. A., Bourqui, M., de Grandpre, J., Hare, S. H. E., Kettleborough, J., Langematz, U., Manzini, E., Sassi, F., Shibata, K., Shindell, D., and Sigmond, M.: Simulations of anthropogenic change in the strength of the Brewer–Dobson circulation, *Clim. Dyn.*, 27, 727-741, 2006.
- 10 Butchart, N., Cionni, I., Eyring, V., Shepherd, T. G., Waugh, D. W., Akiyoshi, H., Austin, J., Brühl, C., Chipperfield, M. P., Cordero, E., Dameris, M., Deckert, R., Dhomse, S., Frith, S. M., Garcia, R. R., Gettelman, A., Giorgetta, M. A., Kinnison, D. E., Li, F., Mancini, E., Mclandress, C., Pawson, S., Pitari, G., Plummer, D. A., Rozanov, E., Sassi, F., Scinocca, J. F., Shibata, K., Steil, B., and Tian, W.: Chemistry-climate model simulations of twenty-first century stratospheric climate and circulation changes, *J. Climate*, 23, 5349–5374, doi:10.1175/2010JCLI3404.1, 2010.
- 15 Chapman, S.: A Theory of Upper-Atmospheric Ozone, *Mem. Roy. Meteorol. Soc.*, 3, 103-125, 1930.
- Chipperfield, M. P. and Feng, W.: Comment on: Stratospheric Ozone Depletion at northern mid-latitudes in the 21st century: The importance of future concentrations of greenhouse gases nitrous oxide and methane, *Geophys. Res. Lett.*, 30, 1389, doi:10.1029/2002GL016353, 2003.
- 20 Chipperfield, M., Liang, Q., Strahan, S., Morgenstern, O., Dhomse, S., Abraham, N., Archibald, A., Bekki, S., Braesicke, P., Di Genova, G., Fleming, E. L., Hardiman, S. C., Iachetti, D., Jackman, C. H., Kinnison, D. E., Marchand, M., Pitari, G., Pyle, J. A., Rozanov, E., Stenke, A., and Tummon, F.: Multimodel estimates of atmospheric lifetimes of long-lived ozone-depleting substances: Present and future, *J. Geophys. Res.-Atmos.*, 119, 2555–2573, 2014.
- Crutzen, P. J.: The influence of nitrogen oxides on the atmospheric ozone content, *Q. J. Roy. Meteorol. Soc.*, 96, 320-325, doi:10.1002/qj.49709640815, 1970.
- 25 Eyring, V., Cionni, I., Bodeker, G. E., Charlton-Perez, A. J., Kinnison, D. E., Scinocca, J. F., Waugh, D. W., Akiyoshi, H., Bekki, S., Chipperfield, M. P., Dameris, M., Dhomse, S., Frith, S. M., Garny, H., Gettelman, A., Kubin, A., Langematz, U., Mancini, E., Marchand, M., Nakamura, T., Oman, L. D., Pawson, S., Pitari, G., Plummer, D. A., Rozanov, E., Shepherd, T. G., Shibata, K., Tian, W., Braesicke, P., Hardiman, S. C., Lamarque, J. F., Morgenstern, O., Pyle, J. A., Smale, D., and Yamashita, Y.: Multi-model assessment of stratospheric ozone return dates and ozone recovery in CCMVal-2 models, *Atmos. Chem. Phys.*, 10, 9451-9472, doi:10.5194/acp-10-9451-2010, 2010.
- 30 Eyring, V., Arblaster, J. M., Cionni, I., Sedláček, J., Perlwitz, J., Young, P. J., Bekki, S., Bergmann, D., Cameron-Smith, P., Collins, W. J., Faluvegi, G., Gottschaldt, K.-D., Horowitz, L. W., Kinnison, D. E., Lamarque, J.-F., Marsh, D. R.,



- Saint-Martin, D., Shindell, D. T., Sudo, K., Szopa, S., and Watanabe, S.: Long-term ozone changes and associated climate impacts in CMIP5 simulations, *J. Geophys. Res.-Atmos.*, 118, 5029-5060, doi:10.1002/jgrd.50316, 2013.
- Farman, J. C., Gardiner, B. G., and Shanklin, J. D.: Large losses of total ozone in Antarctica reveal seasonal ClO_x/NO_x interaction, *Nature*, 315, 207–210, 1985.
- 5 Fleming, E. L., Jackman, C. H., Stolarski, R. S., and Douglass, A. R.: A model study of the impact of source gas changes on the stratosphere for 1850–2100, *Atmos. Chem. Phys.*, 11, 8515-8541, doi:10.5194/acp-11-8515-2011, 2011.
- Forster, P. M. D. F. and Shine, K. P.: Radiative forcing and temperature trends from stratospheric ozone changes, *Geophys. Res. Lett.*, 102, 10 841–10 855, doi:10.1029/96JD03510, 1997.
- Garcia, R. R., Marsh, D. R., Kinnison, D. E., Boville, B. A., and Sassi, F.: Simulation of secular trends in the middle atmosphere, 1950–2003, *J. Geophys. Res.*, 112, D09301, doi:10.1029/2006JD007485, 2007.
- 10 Garny, H., Grewe, V., Dameris, M., Bodeker, G. E., and Stenke, A.: Attribution of ozone changes to dynamical and chemical processes in CCMs and CTMs, *Geosci. Model Dev.*, 4, 271-286, doi:10.5194/gmd-4-271-2011, 2011.
- Groß, J.-U., Müller, R., Becker, G., McKenna, D. S., and Crutzen, P. J.: The upper stratospheric ozone budget: An update of calculations based on HALOE Data, *J. Atmos. Chem.*, 34, 171-183, 1999.
- 15 Haigh, J. D. and Pyle, J. A.: Ozone perturbation experiments in a two-dimensional circulation model, *Q. J. Roy. Meteor. Soc.*, 108, 551–574, doi:10.1002/qj.49710845705, 1982.
- Hall, T. M., and Waugh, D. W.: Timescales for the stratospheric circulation derived from tracers, *J. Geophys. Res.-Atmos.*, 102, 8991–9001, 1997.
- Hardiman, S. C., Butchart, N., and Calvo, N.: The morphology of the Brewer–Dobson circulation and its response to climate change in CMIP5 simulations, *Q. J. Roy. Meteor. Soc.*, 140, 1958–1965, doi:10.1002/qj.2258, 2013.
- 20 Harris, N. R. P., Hassler, B., Tummon, F., Bodeker, G. E., Hubert, D., Petropavlovskikh, I., Steinbrecht, W., Anderson, J., Bhartia, P. K., Boone, C. D., Bourassa, A., Davis, S. M., Degenstein, D., Delcloo, A., Frith, S. M., Froidevaux, L., Godin-Beekmann, S., Jones, N., Kurylo, M. J., Kyrölä, E., Laine, M., Leblanc, S. T., Lambert, J.-C., Liley, B., Mahieu, E., Maycock, A., de Mazière, M., Parrish, A., Querel, R., Rosenlof, K. H., Roth, C., Sioris, C., Staehelin, J., Stolarski, R. S., Stübi, R., Tamminen, J., Vigouroux, C., Walker, K. A., Wang, H. J., Wild, J., and Zawodny, J.
- 25 M.: Past changes in the vertical distribution of ozone – Part 3: Analysis and interpretation of trends, *Atmos. Chem. Phys.*, 15, 9965-9982, doi:10.5194/acp-15-9965-2015, 2015.
- Hewitt, H. T., Copsey, D., Culverwell, I. D., Harris, C. M., Hill, R. S. R., Keen, A. B., McLaren, A. J., and Hunke, E. C.: Design and implementation of the infrastructure of HadGEM3: the next-generation Met Office climate modelling system, *Geosci. Model Dev.*, 4, 223-253, doi:10.5194/gmd-4-223-2011, 2011.
- 30 Iglesias-Suarez, F., Young, P. J., and Wild, O.: Stratospheric ozone change and related climate impacts over 1850–2100 as modelled by the ACCMIP ensemble, *Atmos. Chem. Phys.*, 16, 343-363, doi:10.5194/acp-16-343-2016, 2016.



- PCC: Climate Change 2007: The Physical Science Basis, edited by: Solomon, S., Qin, D., Manning, M., Marquis, M., Averyt, K., Tignor, M. M. B., Miller, H. L., and Chen, Z., Cambridge University Press, Cambridge, UK, 996 pp., 2007.
- IPCC: Climate Change 2013: The Physical Science Basis. Contribution of Working Group I to the Fifth Assessment Report of the Intergovernmental Panel on Climate Change, edited by: Stocker, T. F., Qin, D., Plattner, G.-K., Tignor, M., Allen, S. K., Boschung, J., Nauels, A., Xia, Y., Bex, V., and Midgley, P. M., Cambridge University Press, Cambridge, UK and New York, NY, USA, 2013.
- Johnston, H. S.: Reduction of stratospheric ozone by nitrogen oxide catalysts from supersonic transport exhaust, *Science*, 173, 517-522, 1971.
- 10 Jonsson, A.I., de Grandpre, J., Fomichev, V. I., McConnell, J. C., and Beagley, S. R.: Doubled CO₂-induced cooling in the middle atmosphere: Photochemical analysis of the ozone radiative feedback, *J. Geophys. Res.*, 109, D24103, doi:10.1029/2004JD005093, 2004.
- Keeble, J., Braesicke, P., Abraham, N. L., Roscoe, H. K., and Pyle, J. A.: The impact of polar stratospheric ozone loss on Southern Hemisphere stratospheric circulation and climate, *Atmos. Chem. Phys.*, 14, 13705-13717, doi:10.5194/acp-14-13705-2014, 2014.
- 15 Lamarque, J.-F., Bond, T. C., Eyring, V., Granier, C., Heil, A., Klimont, Z., Lee, D., Liousse, C., Mieville, A., Owen, B., Schultz, M. G., Shindell, D., Smith, S. J., Stehfest, E., Van Aardenne, J., Cooper, O. R., Kainuma, M., Mahowald, N., McConnell, J. R., Naik, V., Riahi, K., and van Vuuren, D. P.: Historical (1850–2000) gridded anthropogenic and biomass burning emissions of reactive gases and aerosols: methodology and application, *Atmos. Chem. Phys.*, 20, 7017–7039, doi:10.5194/acp-10-7017-2010, 2010.
- Li, F., Austin, J., and Wilson, J.: The Strength of the Brewer-Dobson Circulation in a Changing Climate: Coupled Chemistry-Climate Model Simulation, *J. Climate*, 21, 40–57, 2008.
- Lorenz, D. J., and DeWeaver, E. T.: Tropopause height and zonal wind response to global warming in the IPCC scenario intergrations, *J. Geophys. Res.*, 112, D10119, doi:10.1029/2006JD008087, 2007.
- 25 Mäder, J. A., Staehelin, J., Peter, T., Brunner, D., Rieder, H. E., and Stahel, W. A.: Evidence for the effectiveness of the Montreal Protocol to protect the ozone layer, *Atmos. Chem. Phys.*, 10, 12161-12171, doi:10.5194/acp-10-12161-2010, 2010.
- Maycock, A. C.: The contribution of ozone to future stratospheric temperature trends, *Geophys. Res. Lett.*, 43, 4609–4616, doi:10.1002/2016GL068511, 2016.
- 30 Meinshausen, M., Smith, S. J., Calvin, K., Daniel, J. S., Kainuma, M. L. T., Lamarque, J., Matsumoto, K., Montzka, S. A., Raper, S. C. B., Riahi, K., Thomson, A., Velders, G. J. M., and van Vuuren, D. P. P.: The RCP greenhouse gas concentrations and their extensions from 1765 to 2300, *Clim. Change*, 109, 213-241, doi:10.1007/s10584-011-0156-z, 2011.



- Meul, S., Langematz, U., Oberländer, S., Garny, H., and Jöckel, P.: Chemical contribution to future tropical ozone change in the lower stratosphere, *Atmos. Chem. Phys.*, 14, 2959–2971, doi:10.5194/acp-14-2959-2014, 2014.
- Molina, M. J. and Rowland, F. S.: Stratospheric sink for chlorofluoromethanes: chlorine atomcatalysed destruction of ozone, *Nature*, 249, 810–812, doi: 10.1038/249810a0, 1974.
- 5 Morgenstern, O., Braesicke, P., O'Connor, F. M., Bushell, A. C., Johnson, C. E., Osprey, S. M., and Pyle, J. A.: Evaluation of the new UKCA climate-composition model – Part 1: The stratosphere, *Geosci. Model Dev.*, 2, 43–57, doi:10.5194/gmd-2-43-2009, 2009.
- Morgenstern, O., Hegglin, M. I., Rozanov, E., O'Connor, F. M., Abraham, N. L., Akiyoshi, H., Archibald, A. T., Bekki, S., Butchart, N., Chipperfield, M. P., Deushi, M., Dhomse, S. S., Garcia, R. R., Hardiman, S. C., Horowitz, L. W.,
10 Jöckel, P., Josse, B., Kinnison, D., Lin, M., Mancini, E., Manyin, M. E., Marchand, M., Marécal, V., Michou, M., Oman, L. D., Pitari, G., Plummer, D. A., Revell, L. E., Saint-Martin, D., Schofield, R., Stenke, A., Stone, K., Sudo, K., Tanaka, T. Y., Tilmes, S., Yamashita, Y., Yoshida, K., and Zeng, G.: Review of the global models used within phase 1 of the Chemistry–Climate Model Initiative (CCMI), *Geosci. Model Dev.*, 10, 639–671, doi:10.5194/gmd-10-639-2017, 2017.
- 15 Neu, J. L. and Plumb, R. A.: Age of air in a leaky pipe model of stratospheric transport, *Journal of Geophysical Research: Atmospheres*, 104, 19 243–19 255, 1999.
- O'Connor, F. M., Johnson, C. E., Morgenstern, O., Abraham, N. L., Braesicke, P., Dalvi, M., Folberth, G. A., Sanderson, M. G., Telford, P. J., Voulgarakis, A., Young, P. J., Zeng, G., Collins, W. J., and Pyle, J. A.: Evaluation of the new UKCA climate-composition model - Part 2: The Troposphere, *Geosci. Model Dev.*, 7, 41–91, doi:10.5194/gmd-7-41-2014, 2014.
- 20 Oman, L. D., Plummer, D. A., Waugh, D. W., Austin, J., Scinocca, J., Douglass, A. R., Salawitch, R. J., Canty, T., Akiyoshi, H., Bekki, S., Braesicke, P., Butchart, N., Chipperfield, M., Cugnet, D., Dhomse, S., Eyring, V., Frith, S., Hardiman, S. C., Kinnison, D. E., Lamarque, J. F., Mancini, E., Marchand, M., Michou, M., Morgenstern, O., Nakamura, T., Nielsen, J. E., Olivie, D., Pitari, G., Pyle, J., Rozanov, E., Shepherd, T. G., Shibata, K., Stolarski, R.,
25 S., Teyssedre, H., Tian, W., Yamashita, Y., and Ziemke, J. R.: Multi-model assessment of the factors driving stratospheric ozone evolution over the 21st century, *Geophys. Res. Lett.*, 115, D24306, doi:10.1029/2010JD014362, 2010.
- Palmeiro, F. M., Calvo, N., and Garcia, R. R.: Future changes in the Brewer–Dobson circulation under different greenhouse gas concentrations in WACCM4, *J. Atmos. Sci.*, 71, 2962–2975, doi:10.1175/JAS-D-13-0289.1, 2014.
- 30 Plumb, R. A.: A ‘tropical pipe’ model of stratospheric transport, *J. Geophys. Res.*, 101, 3957–3972, 1996.
- Polvani, L. M., Wang, L., Aquila V., and Waugh, D.W.: The impact of ozone depleting substances on tropical upwelling, as revealed by the absence of lower stratospheric cooling since the late 1990s, *J. Climate*, 30, 2523–2534, 2017.



- Randeniya, L. K., Vohralik, P. F., and Plumb, I. C.: Stratospheric ozone depletion at northern mid latitudes in the 21st century: The importance of future concentrations of greenhouse gases nitrous oxide and methane, *Geophys. Res. Lett.*, 29, 1051, doi:10.1029/2001GL014295, 2002.
- Ravishankara, A. R., Daniel, J. S., and Portmann, R. W.: Nitrous Oxide (N₂O): The Dominant Ozone Depleting Substance
5 Emitted in the 21st Century, *Science*, 326(123), 682-125, 2009.
- Revell, L. E., Bodeker, G. E., Huck, P. E., Williamson, B. E., and Rozanov, E.: The sensitivity of stratospheric ozone changes through the 21st century to N₂O and CH₄, *Atmos. Chem. Phys.*, 12, 11309–11317, doi:10.5194/acp-12-11309-2012, 2012.
- Revell, L. E., Tummon, F., Stenke, A., Sukhodolov, T., Coulon, A., Rozanov, E., Garny, H., Grewe, V., and Peter, T.:
10 Drivers of the tropospheric ozone budget throughout the 21st century under the medium-high climate scenario RCP 6.0, *Atmos. Chem. Phys.*, 15, 5887–5902, doi:10.5194/acp-15-5887-2015, 2015.
- Rosenfield, J. E., Douglass, A. R. and Considine, D. B.: The impact of increasing carbon dioxide on ozone recovery, *J. Geophys. Res.*, 107, ACH 7-1–ACH 7-9, doi:10.1029/2001JD000824, 2002.
- Shepherd, T. and McLandress, C.: A robust mechanism for strengthening of the Brewer-Dobson circulation under climate
15 change: Critical-layer control of subtropical wave breaking, *J. Atmos. Sci.*, 68, 784–797, 2011.
- Shepherd, T. G.: Dynamics, stratospheric ozone, and climate change, *Atmos. Ocean*, 46, 117–138, 2008.
- Shine, K. P., Bourqui, M. S., Forster, P. M. F., et al.: A comparison of model-simulated trends in stratospheric temperature, *Q. J. R. Met. Soc.*, 129, 1565–1588, doi:10.1256/qj.02.186, 2003.
- Solomon, S., Portmann, R., Garcia, R. R., Thomason, L., Poole, L. R., and McCormick, M. P.: The role of aerosol variations
20 in anthropogenic ozone depletion at northern midlatitudes, *J. Geophys. Res.*, 101, 6713–6727, 1996.
- SPARC: SPARC Report on the Lifetimes of Stratospheric Ozone-Depleting Substances, Their Replacements, and Related Species, Edited by M.K.W. Ko, P.A. Newman, S. Reimann, and S.E. Strahan, SPARC Report No. 6, WCRP-15/2013, 2013.
- Stolarski, R. S. and Cicerone, R. J.: Stratospheric chlorine: a possible sink for ozone, *Can. J. Chem.* 52, 1610-1615, 1974.
- 25 Stolarski, R. S., Douglass, A. R., Oman, L. D., and Waugh, D. W.: Impact of future nitrous oxide and carbon dioxide emissions on the stratospheric ozone layer, *Environ. Res. Lett.*, 10, 034011, doi:10.1088/1748-9326/10/3/034011, 2015.
- Tang, M., Keeble, J., Telford, P. J., Pope, F. D., Braesicke, P., Griffiths, P. T., Abraham, N. L., McGregor, J., Watson, I. M., Cox, R. A., Pyle, J. A., and Kalberer, M.: Heterogeneous reaction of ClONO₂ with TiO₂ and SiO₂ aerosol
30 particles: implications for stratospheric particle injection for climate engineering, *Atmos. Chem. Phys.*, 16, 15397-15412, doi:10.5194/acp-16-15397-2016, 2016.
- Telford, P. J., Braesicke, P., Morgenstern, O., and Pyle, J.: Reassessment of causes of ozone column variability following the eruption of Mount Pinatubo using a nudged CCM, *Atmos. Chem. Phys.*, 9, 4251–4260, doi:10.5194/acp-9-4251-2009, 2009.



- Thompson, A. M., Stewart, R. W., Owens, M. A., and Herwehe, J. A.: Sensitivity of tropospheric oxidants to global chemical and climate change, *Atmospheric Environment*, 23, 519-532, 10.1016/0004-6981(89)90001-2, 1989.
- van Vuuren, D. P., Edmonds, J., Kainuma, M., Riahi, K., Thomson, A., Hibbard, K., Hurtt, G. C., Kram, T., Krey, V., Lamarque, J.-F., Masui, T., Meinshausen, M., Nakicenovic, N., Smith, S. J., and Rose, S. K.: The representative concentration pathways: an overview, *Clim. Change*, 109, 5–31, doi:10.1007/s10584-011-0148-z, 2011.
- 5 Waugh, D. W.: Seasonal variation of isentropic transport out of the tropical stratosphere, *J. Geophys. Res.-Atmos.*, 101, 4007–4023, doi:10.1029/95JD03160, 1996.
- Weisenstein, D. K., Keith, D. W., and Dykema, J. A.: Solar geoengineering using solid aerosol in the stratosphere, *Atmos. Chem. Phys.*, 15, 11835–11859, doi:10.5194/acp-15-11835-2015, 2015.
- 10 World Meteorological Organization (WMO): Scientific Assessment of Ozone Depletion: 2014, Global Ozone Research and Monitoring Project, Report No. 55, Geneva, Switzerland, 2014.
- World Meteorological Organisation (WMO): *Meteorology – a three-dimensional science*, *WMO Bull.*, 6, 134–138, 1957.
- World Meteorological Organization (WMO): Scientific Assessment of Ozone Depletion: 1998, Global Ozone Research and Monitoring Project, Report No. 44, Geneva, Switzerland, 1999.
- 15 World Meteorological Organization (WMO): Scientific Assessment of Ozone Depletion: 2010, Global Ozone Research and Monitoring Project, Report No. 52, Geneva, Switzerland, 2011.
- Young, P. J., Archibald, A. T., Bowman, K. W., Lamarque, J.-F., Naik, V., Stevenson, D. S., Tilmes, S., Voulgarakis, A., Wild, O., Bergmann, D., Cameron-Smith, P., Cionni, I., Collins, W. J., Dalsøren, S. B., Doherty, R. M., Eyring, V., Faluvegi, G., Horowitz, L. W., Josse, B., Lee, Y. H., MacKenzie, I. A., Nagashima, T., Plummer, D. A., Righi, M., Rumbold, S. T., Skeie, R. B., Shindell, D. T., Strode, S. A., Sudo, K., Szopa, S., and Zeng, G.: Pre-industrial to end 21st century projections of tropospheric ozone from the Atmospheric Chemistry and Climate Model Intercomparison Project (ACCMIP), *Atmos. Chem. Phys.*, 13, 2063-2090, doi:10.5194/acp-13-2063-2013, 2013.
- 20 Zeng, G. and Pyle, J. A.: Changes in tropospheric ozone between 2000 and 2100 modeled in a chemistry-climate model, *Geophys. Res. Lett.*, 30, 1392, doi:10.1029/2002GL016708, 2003.



Simulation name	Climate (SST, sea ice, GHG)	ODS (Cl _y , Br _y)
TS2000	2000	2000
TS2000 _{ODS}	2000	2100 (RCP4.5)
TS4.5	2100 (RCP4.5)	2000
TS4.5 _{ODS}	2100 (RCP8.5)	2100 (RCP4.5)
TS8.5	2100 (RCP4.5)	2000
TS8.5 _{ODS}	2100 (RCP8.5)	2100 (RCP4.5)

Table 1. Simulation names and corresponding climate (including radiative impacts of GHGs, SSTs and sea ice) and ODS loadings. RCP scenario used for future GHG and ODS concentrations given in parentheses.



	Integration	PCO ₃	Lifetime	Production	Loss	Halogens	HO _x	NO _x	O _x
PCO _{3,US}	TS2000	63 DU	1 day	48 DU day ⁻¹	48 DU day ⁻¹	9 DU day ⁻¹	11 DU day ⁻¹	19 DU day ⁻¹	9 DU day ⁻¹
	TS2000 _{ODS}	+8%	+13%	-5%	-5%	-63%	+9%	+4.5%	+19%
	TS4.5	+5%	+8%	-3%	-3%	+2%	+2%	-5%	-7%
	TS8.5	+19%	+27%	-6%	-6%	+4%	+11%	-13%	-21%
PCO _{3,LS}	TS2000	179 DU	34 days	7 DU day ⁻¹	5 DU day ⁻¹	1 DU day ⁻¹	2 DU day ⁻¹	2 DU day ⁻¹	1 DU day ⁻¹
	TS2000 _{ODS}	+4%	+21%	-10%	-14%	-65%	-6%	+3%	+7%
	TS4.5	-3%	+8%	-8%	-10%	-5%	-8%	-10%	-8%
	TS8.5	-7%	+23%	-16%	-25%	-17%	-15%	-33%	-37%

Table 2. Partial column ozone values (DU), average ozone lifetime (days), net chemical production and loss and absolute contribution of halogen, HO_x, NO_x and O_x ozone destroying cycles (DU day⁻¹) in the upper and lower stratospheric for the TS2000 integration. Percentage differences are given for the TS2000_{ODS}, TS4.5 and TS8.5 simulations relative to the TS2000 integration.

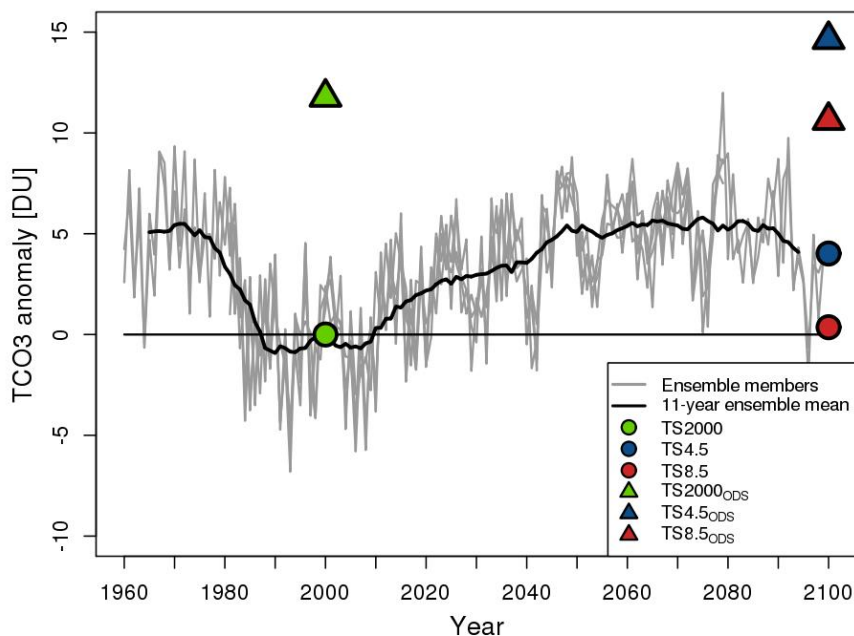


Figure 1. Total column ozone anomalies (in DU) relative to the year 2000 ± 5 mean, averaged over 10°S - 10°N for the four transient UM-UKCA experiments following the RCP6.0 future emissions scenario (grey lines), and the ensemble mean 11-year running mean (black line). Coloured circles and triangles represent tropical total column ozone in the time-slice experiments, as given in the figure legend.

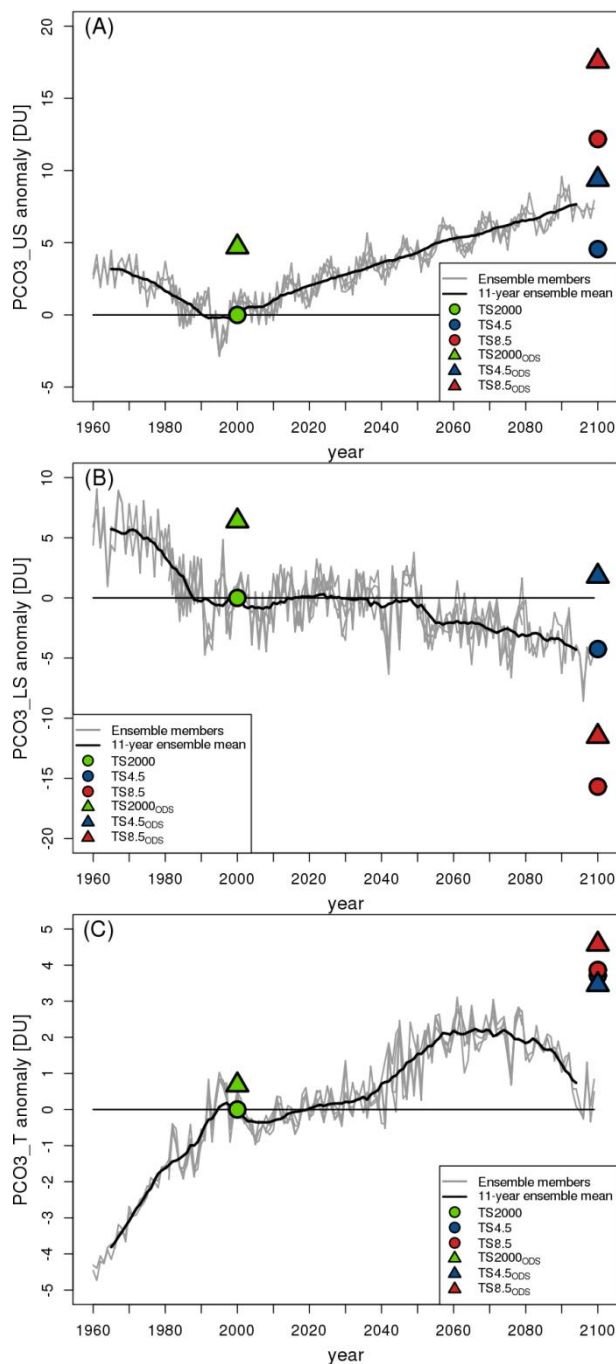


Figure 2. As for Figure 1, but for partial columns for (a) the upper stratosphere (30-48 km), (b) lower stratosphere (tropopause-30 km) and (c) troposphere.

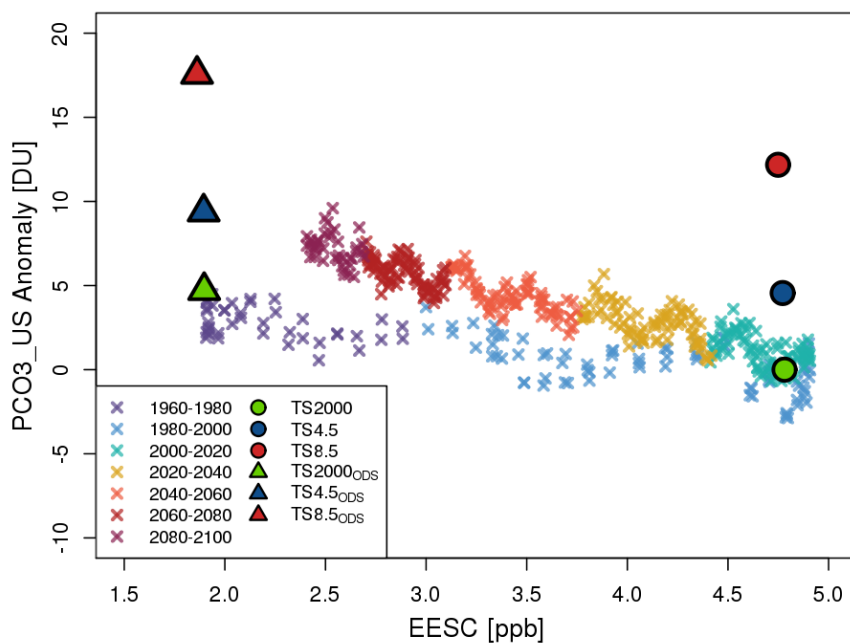


Figure 3. Scatterplot of annual mean upper stratospheric partial column ozone anomalies relative to the year 2000±5 mean (in DU) vs. 45km EESC (in ppb) for the transient simulation (crosses) and time slice experiments (circles and triangles). Results from the transient simulations have been coloured in 20 year sections.

5

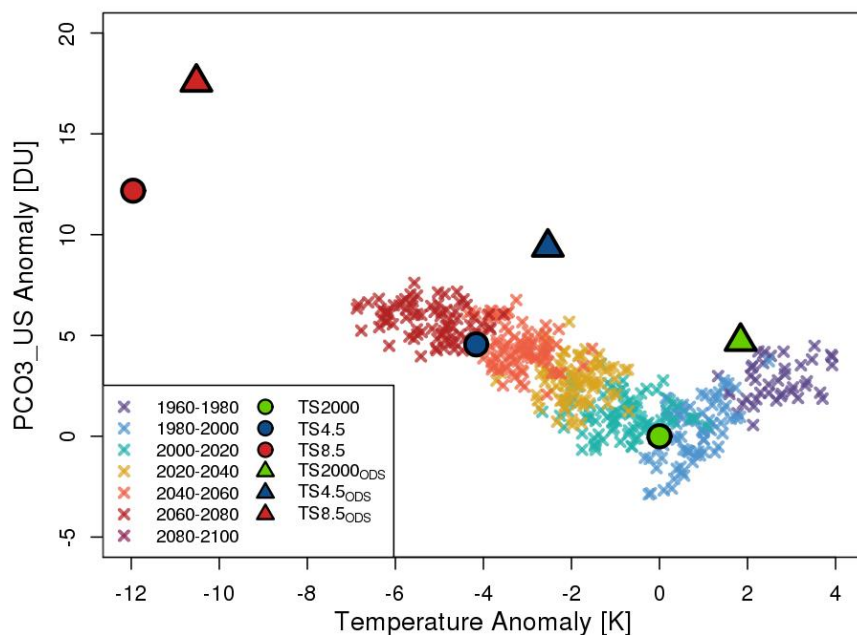


Figure 4. Scatterplot of annual mean upper stratospheric partial column ozone anomalies relative to the year 2000 ± 5 mean (in DU) vs. 45km temperature (in K) for the transient simulation (crosses) and time slice experiments (circles and triangles). Results from the transient simulations have been coloured in 20 year sections.

5

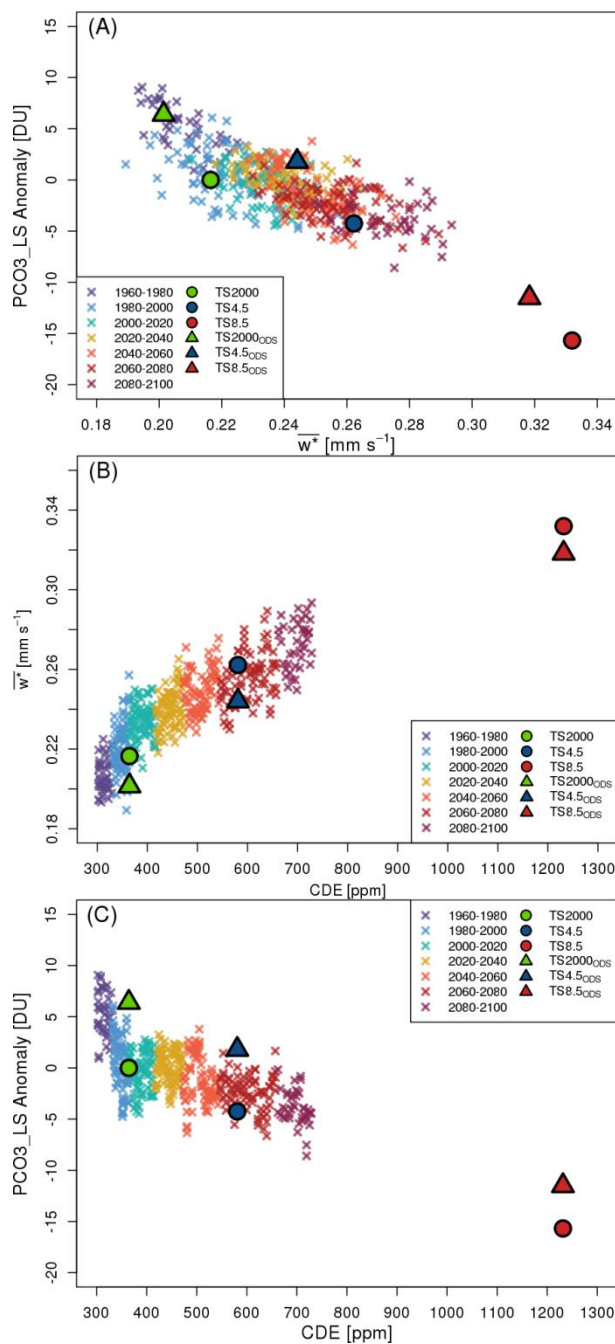


Figure 5. Scatterplot of (a) lower stratospheric partial column ozone anomalies relative to the year 2000±5 mean (in DU) vs 70hPa $\overline{w^*}$ (in mm/s), (b) 70hPa $\overline{w^*}$ vs CDE mixing ratio (in ppmv) and (c) lower stratospheric partial column ozone



anomalies vs CDE mixing ratio for the transient simulations (crosses) and time slice experiments (circles and triangles). Results from the transient simulations have been coloured in 20 year sections.

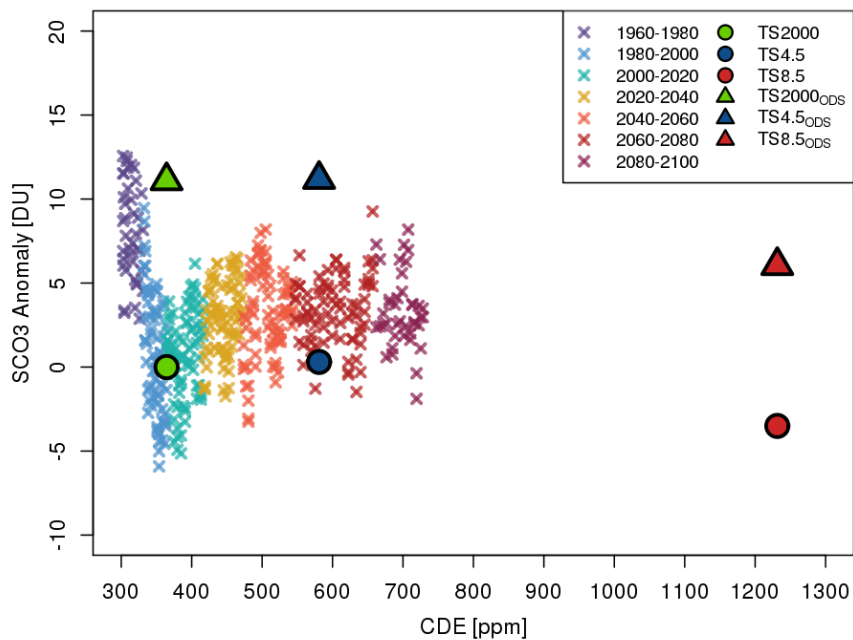


Figure 6. Scatterplot of stratospheric column ozone anomalies relative to the year 2000±5 mean (in DU) vs CO₂ mixing ratio (in ppmv) for the transient simulation (crosses) and time slice experiments (circles and triangles). Results from the transient simulations have been coloured in 20 year sections.

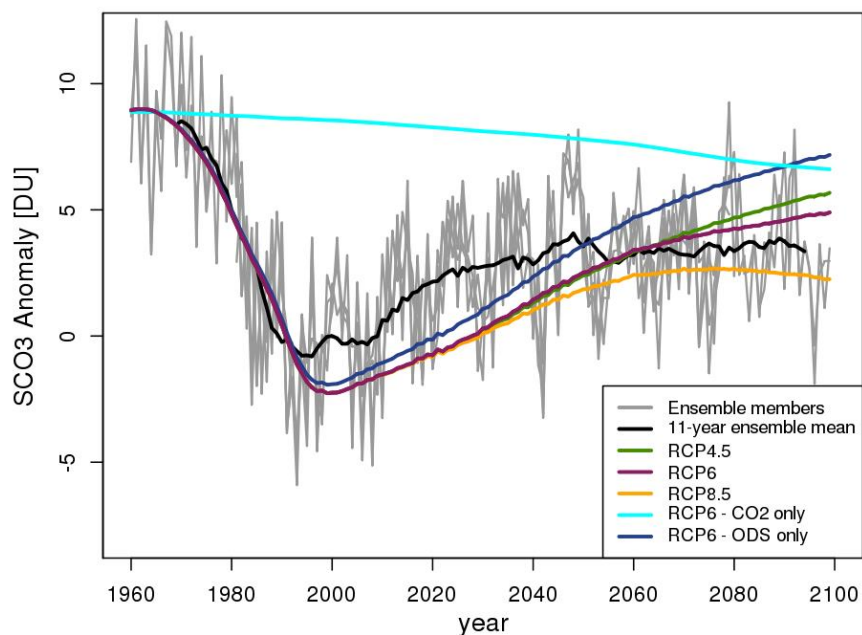


Figure 7. Annual mean stratospheric column ozone anomalies relative to the year 2000 ± 5 mean (in DU) as modelled by the transient simulations (grey lines), with the ensemble mean 11-year running mean also plotted (black line). Results obtained using the simple model are shown for a range of emissions scenarios, initialised to 1960 values taken from the transient run.